Bioresource Technology 102 (2011) 3155–3162

Contents lists available at ScienceDirect

Bioresource Technology

journal homepage: www.elsevier.com/locate/biortech

Mathematical modeling of hydrolysate diffusion and utilization in cellulolytic biofilms of the extreme thermophile *Caldicellulosiruptor obsidiansis*

Zhi-Wu Wang, Scott D. Hamilton-Brehm, Adriane Lochner, James G. Elkins *, Jennifer L. Morrell-Falvey *

BioEnergy Science Center, Biosciences Division, Oak Ridge National Laboratory, Oak Ridge, TN 37831, USA

ARTICLE INFO

Article history:
Received 9 July 2010
Received in revised form 20 October 2010
Accepted 21 October 2010
Available online 28 October 2010

Keywords:
Thermophile
Biofilm
Cellulose
Diffusion
Biofuel

ABSTRACT

In this study, a hydrolysate diffusion and utilization model was developed to examine factors influencing cellulolytic biofilm morphology. Model simulations using *Caldicellulosiruptor obsidiansis* revealed that the cellulolytic biofilm needs to generate more hydrolysate than it consumes to establish a higher than bulk solution intra-biofilm substrate concentration to support its growth. This produces a hydrolysate surplus that diffuses through the thin biofilm structure into the bulk solution, which gives rise to a uniform growth rate and hence the homogeneous morphology of the cellulolytic biofilm. Model predictions were tested against experimental data from a cellulose-fermenting bioreactor and the results were consistent with the model prediction and indicated that only a small fraction (10–12%) of the soluble hydrolysis products are utilized by the biofilm. The factors determining the rate-limiting step of cellulolytic biofilm growth are also analyzed and discussed.

1. Introduction

The simultaneous solubilization and fermentation of lignocellulosic biomass into alcohols through a consolidated bioprocess would improve the economics of renewable fuel production (Lynd et al., 2008). While much has been described regarding the enzymes employed by microbes to access carbohydrates derived from biomass (Bayer et al., 2006; Himmel et al., 2010), other surface related phenomena remain poorly characterized. Some microorganisms that efficiently degrade biomass and convert the hydrolysate into fermentation end-products form biofilms (Jensen et al., 2009; O'Sullivan et al., 2009; Wang and Chen, 2009). Microbial biofilms demonstrate diverse morphological and structural characteristics under different cultivation conditions (van Loosdrecht et al., 2002). In general, the processes of internal mass diffusion and utilization play an important role in shaping the morphology of biofilms, such that the biofilm structure will tend to become heterogeneous and porous when substrate diffusion is rate-limiting, but homogeneous and compact when substrate utilization becomes the rate-limiting step (van Loosdrecht et al., 2002). This holds true for both pure and mixed cultures (Park et al., 1998; Trulear and Characklis, 1982).

Many studies of cellulose-degrading microbes have described the formation of biofilms with thin and uniform morphologies (Miron et al., 2001; Weimer et al., 1993). The underlying mechanisms that may constrain the morphology of cellulolytic biofilms, however, remain unknown. Unlike well-characterized biofilms that feed on soluble substrates, cellulolytic microbes must first hydrolyze the cellulose substrate and then utilize the hydrolysate for growth. In environments where cellulose is the primary carbon source, growth and survival of non-cellulolytic bacteria alongside cellulolytic microorganisms is thought to be supported by hydrolysate cross-feeding (Scheifinger and Wolin, 1973; Wells et al., 1995). This explanation requires that the rate of substrate hydrolysis and diffusion in a cellulolytic biofilm is faster than the rate of hydrolysate utilization by the biofilm, though this prediction has not been fully tested. Previous studies regarding cellulose fermentation by microbes, however, suggest that substrate hydrolysis is the rate-limiting step in a system which includes both attached and non-attached cellulolytic bacteria (Lynd et al., 2002). To provide additional insight into cellulolytic biofilm formation and growth, a mathematical model for substrate utilization and diffusion kinetics is described based on calculated and experimentally-derived parameters using *Caldicellulosiruptor obsidiansis* (ATCC BAA-2073) as a representative microorganism. *C. obsidiansis* is a recently described, extremely thermophilic and cellulolytic microbe isolated from Obsidian Pool in Yellowstone National Park. This microorganism has the capacity to utilize both cellulose and xylan while fermenting hexose and pentose sugars to lactate, acetate, ethanol, hydrogen and carbon dioxide (Hamilton-Brehm et al., 2010). Members of the genus *Caldicellulosiruptor* are known to express heat-stable multifunctional/multidomain cellulases and hemicellulases that act in concert to hydrolyze plant biomass

* Corresponding authors. Tel.: +1 865 241 2841; fax: +1 865 574 5345 (J.L. Morrell-Falvey), tel.: +1 865 241 1386; fax: +1 865 576 8646 (J.G. Elkins).
E-mail addresses: elkinsjg@ornl.gov (J.G. Elkins), morrelljl1@ornl.gov (J.L. Morrell-Falvey).

0960-8524/$ - see front matter © 2010 Elsevier Ltd. All rights reserved.
doi:10.1016/j.biortech.2010.10.104

(Bayer et al., 2006). Model simulations in this study suggest that hydrolysate utilization by the cellulolytic biofilm is the rate-limiting step for *C. obsidiansis* biofilm growth.

2. Methods

2.1. Experimental design

C. obsidiansis was isolated and cultured in serum bottles as described previously (Hamilton-Brehm et al., 2010). Regenerated amorphous cellulose membranes with 0.2 μm pore size (Whatman RC58, Maidstone, Kent, UK) were used as a model substrate in this study. Identical chads with a mean diameter of 7.37 ± 0.03 mm and weight equal to 1.60 ± 0.14 mg were stamped from the membrane and used as the sole carbon source for *C. obsidiansis* growth. One cellulose chad was added to 50 ml of nutrient medium without yeast extract in an anaerobic serum bottle, inoculated with 2×10^5 cells ml^{-1}, and incubated at 75 °C on a 100 rpm shaker. This gives an equivalent to 0.03 g L^{-1} of initial cellulose concentration. This low initial cellulose concentration was intentionally designed to avoid accumulation of bulk solution hydrolysate to the extent necessary to support planktonic cell growth. This is confirmed by undetectable levels of reducing sugar and lack of dividing cells in the bulk solution during the experiment (data not shown). Replicate serum bottles were prepared and 3 serum bottles were randomly sampled and sacrificed for analysis every 4 h and the results from each time point were averaged. For the Avicel fermentation, the fermentor setup and growth conditions were as reported previously (Hamilton-Brehm et al., 2010), except that 30 g L^{-1} rather than 15 g L^{-1} of Avicel was used in this study.

2.2. Intrinsic kinetic parameters determination

Serum bottles containing nutrient medium and varying cellobiose concentrations (0–4 g L^{-1}) were inoculated with approx. 1.0×10^7 cells ml^{-1}. The serum bottles were incubated at 75 °C and sampled every 2 h for 24 h to determine mid-log phase specific growth rates for each respective cellobiose concentration. The maximum specific growth rate (μ_{max}) and half saturation constant (K_s) were regressed with the Monod equation from the cellobiose concentration-dependent specific growth rate plot. The observed growth yield (Y_{obs}) was calculated by measuring the log-phase cellobiose consumption and *C. obsidiansis* cell growth. All experiments were performed in triplicate.

2.3. Microscopic analysis

Cellulose chads were collected from serum bottles and stained with Syto 9, a fluorescent nucleic acid dye (Invitrogen, Carlsbad, CA), to visualize the distribution of *C. obsidiansis* cells using a confocal laser scanning microscope (Leica TCS SP2, Mannheim, Germany). The mean thickness of each cellulose chad was determined by measuring the change in the *Z* dimension based on focusing the confocal microscope on the top and bottom of the chad at 10 randomly chosen positions. Biofilm thickness was measured from the cross-sectional image. The planktonic cell concentration was determined using a Thoma cell counting chamber (Blaubrand, Wertheim, Germany) and an Axioskop2 Plus microscope (Zeiss, Thornwood, NY, USA) with phase contrast illumination. ImageJ software (Version 1.42q, NIH, Bethesda, MD) was used for image analysis. The ImageJ 3D viewer and 3D object counter plug-ins were utilized to reconstruct the biofilm 3D structure and determine the biofilm cell density.

2.4. Analytical methods

Samples collected from the fermentation were immediately stored at 4 °C and analyzed within 24 h. The concentration of reducing sugars in the growth medium was determined using dinitrosalicylic acid (DNS) reagent according to (Miller, 1959). Briefly, each *C. obsidiansis* fermentation sample was centrifuged at 16,060×*g* for 5 min and the supernatant was then passed through a 0.22 μm nylon filter (PALL, Port Washington, NY) to remove residual cells. DNS reagent (100 μl) was added to 50 μl of filtered supernatant in a 96 well, 0.2 ml thin wall plate, which was sealed with an aluminium microplate seal and incubated in a thermal cycler at 99 °C for 5 min. Fifty microlitres of the reaction mixture was then transferred to a 96 well optical bottom plate (NUNC, Thermo Scientific, Rochester, NY) and diluted with 100 μl of deionized water. The absorbance was read at 540 nm and the amount of reducing sugars calculated as glucose equivalents, based on a glucose standard curve. The densities of the cellulose chads were measured according to standard methods (APHA, 1998). The residual Avicel was measured gravimetrically as previously described (Hamilton-Brehm et al., 2010). All measurements were done in triplicate.

2.5. Modeling parameters

2.5.1. Model description and assumptions

In general, a cellulolytic biofilm consists of four compartments: (i) cellulose substratum, (ii) microbial biofilm, (iii) diffusional boundary layer and (iv) bulk solution (Fig. 1). The primary objective of this model was to describe the hydrolysate transport and conversion within the biofilm and the boundary layer compartments. The hydrolysate is assumed to be produced at the cellulose-biofilm interface and utilized for microbial growth as it diffuses through the biofilm at a given influx of J_{in} (M L^{-2} T^{-1}). Surplus hydrolysate, if any, diffuses through the biofilm into the boundary layer at an efflux of $J_{f\text{-}out}$. If the hydrolysate is not completely consumed in the boundary layer by cells that detached from the biofilm surface, a residual boundary layer substrate flux, namely $J_{b\text{-}out}$, would leak into the bulk solution. Given these hydrolysate flux definitions, the fraction of substrate utilization by the cellulolytic biofilm and boundary layer, can be reflected by the expressions $(J_{in} - J_{f\text{-}out})/J_{in}$ and $(J_{f\text{-}out} - J_{b\text{-}out})/J_{in}$, respectively. In addition, $J_{b\text{-}out}/J_{in}$ reflects the percent of hydrolysate leakage into the bulk solution. Cellobiose, a dimer of two glucose molecules, was chosen as the model substrate in this study because it is a

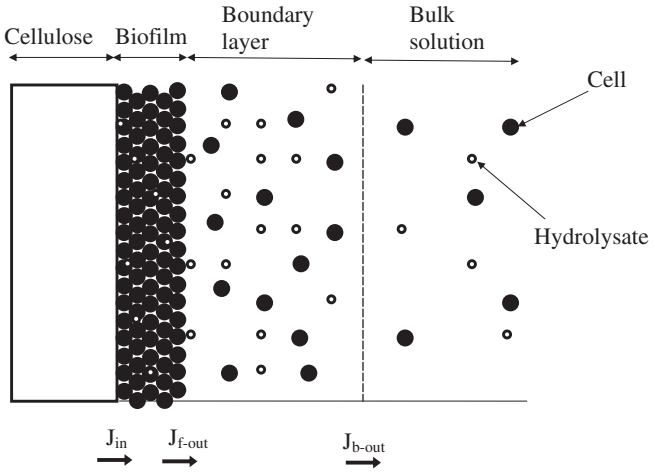

Fig. 1. Schematic representation of the cellulolytic biofilm system.

common growth substrate for cellulolytic bacteria. Also, the growth rate does not appear to differ greatly when using cellobiose versus other cellodextrins (Russell, 1985). The following assumptions were made in the development of the cellulolytic biofilm model: (1) Only cells in the biofilm are responsible for substrate hydrolysis; (2) the biofilm structure is isotopic in physical, chemical and biological properties; (3) the bulk solution is homogeneously mixed; and (4) cellulose (and not other nutrients) is the limiting factor for biofilm growth.

2.5.2. Modeling substrate diffusion and utilization in biofilm and boundary layer

Because the hydrolysate will be at least partially consumed as it diffuses through the biofilm, a diffusion flux reduction should occur which can be described according to Fick's second law and expressed as,

$$(-D_e)\frac{d^2S}{dL^2} = v \tag{1}$$

in which v is the hydrolysate flux reduction rate ($M\,L^{-3}\,T^{-1}$), S is the hydrolysate concentration ($M\,L^{-3}$), D_e is the effective substrate diffusion coefficient inside the biofilm ($L^2\,T^{-1}$) and L is the perpendicular distance from cellulose surface. The substrate utilization kinetics in a biofilm are defined in the same manner as with planktonic cells but the internal soluble substrate concentration is adjusted to reflect the environment near the attached cells (Rittmann and McCarty, 2001). Thus, the substrate utilization rate in a cellulolytic biofilm can be expressed with the Monod equation,

$$v = \frac{\rho_x}{Y_{obs}}\frac{\mu_{max}S}{K_s + S} \tag{2}$$

in which ρ_x is the biofilm cell density ($M\,L^{-3}$), μ_{max} and K_s are the maximum specific growth rate (T^{-1}) and half-reaction constant ($M\,L^{-3}$), and Y_{obs} is the observed growth yield of *C. obsidiansis* cells ($M\,M^{-1}$). Substituting Eqs. (2) into (1) gives the following expression that describes substrate diffusion and utilization in a cellulolytic biofilm:

$$(-D_e)\frac{d^2S}{dL^2} = \frac{\mu_{max}S}{K_s + S}\frac{\rho_x}{Y_{obs}} \tag{3}$$

Substrate utilization in the boundary layer is rarely considered in models for biofilms growing on soluble substrates, which is probably because the boundary layer is very thin compared to the thickness of the biofilm layer (Rittmann and McCarty, 2001). Because of the thin structure of the cellulolytic biofilm, however, the significance of this parameter was investigated further. Similar to the equations above, the substrate diffusion and utilization in the boundary layer can be described by,

$$(-D)\frac{d^2S}{dL^2} = \frac{\mu_{max}S}{K_s + S}\frac{X_b}{Y_{obs}} \tag{4}$$

where D is the hydrolysate diffusion coefficient in water ($L^2\,T^{-1}$) and X_b is the cell concentration within the boundary layer.

2.5.3. Modeling cell diffusion in the boundary layer

A fraction of the attached cells should detach from the cellulolytic biofilm surface and migrate across the boundary layer into the bulk liquid. Different from substrate diffusion, the flux of cells into the bulk solution might increase due to cell growth and division during detachment and diffusion. Therefore, the diffusion and growth of those detached cells in the boundary layer should also follow Fick's second law and Monod equation in the same manner as in Eq. (4), i.e.,

$$D_x\frac{d^2X}{dL^2} = \frac{\mu_{max}S}{K_s + S}X_b \tag{5}$$

where D_x is the cell diffusion coefficient ($L^2\,T^{-1}$).

2.5.4. Boundary conditions

To solve Eqs. (3)–(5) requires the definition of several boundary conditions. For Eq. (3), the substrate flux into the biofilm at its interface with the cellulose surface can be described according to Fick's first law,

$$(-D_e)\frac{dS}{dL} = J_{in} \tag{6}$$

The substrate efflux from the biofilm, if any, should be continuous at the interface between the biofilm and the boundary layer, and so is the substrate concentration. Accordingly,

$$(-D_e)\left.\frac{dS}{dL}\right|_{L=L_f^-} = (-D)\left.\frac{dS}{dL}\right|_{L=L_f^+} \tag{7}$$

$$S|_{L=L_f^-} = S|_{L=L_f^+} \tag{8}$$

in which L_f is the biofilm thickness. L_f^+ and L_f^- are the perpendicular distance measured from the inner and outer side of the biofilm-boundary layer interface to the cellulose surface, respectively. Eq. (4) shares the boundary conditions derived from Eqs. (7) and (8) with Eq. (3). The same concept applies to the boundary layer-bulk solution interface, where

$$(-D)\left.\frac{dS}{dL}\right|_{L=L_f+L_b} = J_{b-out} \tag{9}$$

$$S|_{L=L_f+L_b} = S_s \tag{10}$$

in which S_s is the supernatant hydrolysate concentration ($M\,L^{-3}$), and L_b refers to the boundary layer thickness.

In Eq. (5), the planktonic cell concentration and the cell detachment rate measured in the bulk solution can be used to define the boundary conditions at the interface between the boundary layer and bulk liquid,

$$D\left.\frac{dX}{dL}\right|_{L=L_f+L_b} = \frac{R_{det}V}{A} \tag{11}$$

$$X|_{L=L_f+L_b} = X_p \tag{12}$$

in which R_{det}, V, A and X_p stand for the bacterial detachment rate ($M\,L^{-3}\,T^{-1}$), bulk solution volume (L^3) and the surface area (L^2) of cellulose that is covered by the biofilm and the planktonic cell concentration ($M\,L^{-3}$), respectively.

To solve differential Eqs. (3) and (4), at least two of the boundary conditions defined in Eqs. 6, 9, and 10 must be known in view of the function continuity in Eqs. (7) and (8). In addition, the value X_b in differential Eq. (4) relies on the solution from differential Eq. (5) which can be solved only when both Eqs. (11) and (12) are known. More importantly, since differential Eqs. (3)–(5) share common variables such as S and X_b that vary at different L, these three differential equations must be solved simultaneously. Due to this complexity, Matlab R2009a was used to determine numerical solutions to these equations.

2.5.5. Estimation of other modeling parameters

The crowded cellular environment in a cellulolytic biofilm creates resistance for hydrolysate diffusion. The biofilm cell density dependent mass diffusion coefficient has been recognized and quantified with an empirical model developed by Fan et al. (1990), and expressed as,

$$\frac{D_e}{D} = 1 - \left[\frac{0.43(m_c\rho_x)^{0.92}}{11.19 + 0.27(m_c\rho_x)^{0.99}}\right] \quad (13)$$

in which m_c denotes the single cell dry mass (Table 1). D_e/D is estimated to be 0.18 in this study (Table 1). This ratio is within the range reported for biofilms at comparable cell density (Stewart, 1998). The temperature dependent D value can be converted through the Stokes–Einstein equation. D_x is chosen from published reports for cells with similar morphology to *C. obsidiansis* without mobility (Kim, 1996). To date, no reliable method for estimating the boundary layer thickness (L_b) on a suspended particle in a bulk solution has been reported. In order to determine an appropriate value for L_b, a wide range of values were chosen as input for the model system and the simulation results were compared to experimental data to determine an appropriate value. All other parameters used in this model are listed in Table 1.

3. Results and discussion

3.1. Morphology of the cellulolytic biofilm grown on cellulose chad surfaces

One cellulose chad was sampled and stained with Syto9 to determine the morphology of the *C. obsidiansis* biofilm after 68 h growth using confocal microscopy. Optical sections were collected and used to reconstruct a 3-dimensional image of the biofilm growing on the cellulose substrate (data not shown). The thickness of this biofilm was randomly measured at various positions and found to be in the range of 9–11 μm. After the first 20 h of growth, the maximum thickness of the biofilm remained constant until the end of the experiment (72 h) and cross-sections showed that *C. obsidiansis* cells were evenly distributed throughout the biofilm (data not shown). Moreover, the biofilm did not display any obvious porosity or mushroom-like structures commonly seen in biofilms grown on soluble substrates (van Loosdrecht et al., 2002). This uniform morphology suggests that the substrate concentration is in a state of homogeneous distribution throughout the biofilm. To test this hypothesis, a model was developed to describe the hydrolysate diffusion and utilization in cellulolytic biofilm.

3.2. Modeling hydrolysate diffusion and utilization in a cellulolytic biofilm

During biofilm formation, thinning of the cellulose chad was observed, which is consistent with the chad being used as a carbon source for microbial growth. The reduction in chad thickness due to microbial degradation was determined at multiple time points during the 72 h experiment (Fig. 2A). Thinning of the chad was first observed after 28 h of growth (Fig. 2A). From this point, the cellulose chad thickness decreased at a relatively steady rate (Fig. 2A). This rate of thinning was independent of the planktonic cell concentration measured in the bulk liquid (Fig. 2B), suggesting that the thinning was due to a constant rate of substrate hydrolysis by attached cells but not planktonic cells, which is consistent with published reports (Jensen et al., 2009). From these data, the hydrolysate flux per chad surface area into the biofilm in Eq. (6) can be approximated as,

$$J_{in} = \rho_c R_{thi} \quad (14)$$

in which ρ_c is the cellulose chad density, and R_{thi} is the chad thinning rate estimated from Fig. 2A. Because the initial experimental conditions were designed to prevent planktonic cell growth, the cell detachment rate per surface area (R_{det}) can be estimated from Fig. 2B at the stage when the cellulose chad surface was fully covered by the cellulolytic biofilm, namely after 40 h incubation as observed by microscopy, and substituted into Eq. (11). Similarly, the substrate concentration in the bulk liquid (S_s) in Eq. (10) is negligible based on the experimental design. Further, the value of X_p in Eq. (12) was also determined experimentally (Fig. 2B). Using these values, the hydrolysate diffusion and utilization model was numerically solved with these four boundary conditions at various scales of L_b (Table 2). The specific biofilm growth rate (μ_f) in Table 2 is calculated from the model through a mass balance of biofilm growth, i.e.,

Table 1
Experimental and modeling parameters.

Symbol	Description	Values	Units	References
ρ_x	Biofilm cell density	1.69×10^{11}	cells cm^{-3}	This study
ρ_c	Cellulose chad density	289.07 ± 3.22	kg m^{-3}	This study
D_e	Effective diffusion coefficient	0.18 × D	cm^2 s^{-1}	This study
D (75 °C)	Cellobiose diffusion coefficient	1.38×10^{-5}	cm^2 s^{-1}	This study
D (30 °C)		5.71×10^{-6}	cm^2 s^{-1}	(Kurath and Swanson, 1961)
D_x (75 °C)	Cell diffusion coefficient	2.18×10^{-5}	cm^2 s^{-1}	This study
D_x (28 °C)		9×10^{-6}	cm^2 s^{-1}	(Kim, 1996)
μ_f	Biofilm specific growth rate	0.13	h^{-1}	This study
μ_{max}	Maximum specific growth rate	0.72	h^{-1}	This study
K_s	Half-reaction coefficient	0.38	g L^{-1}	This study
Y_{obs}	Observed growth yield	3.40×10^{12}	cells g^{-1}	This study
L_f	Biofilm thickness	10	μm	This study
A	Cellulose chad surface area	85.28	mm^2	This study
J_{in}	Hydrolysate flux into biofilm	5.33×10^{-5}	g h^{-1} cm^{-2}	This study
$J_{f\text{-}out}$	Hydrolysate flux out of biofilm		g h^{-1} cm^{-2}	This study
$J_{b\text{-}out}$	Hydrolysate flux out of boundary layer		g h^{-1} cm^{-2}	This study
V	Medium volume	50	ml	This study
R_{det}	Detachment rate	4.59×10^5	cells ml^{-1} h^{-1}	This study
R_{thi}	Chad thinning rate	3.69	μm h^{-1}	This study
m_{cell}	Cellular unit dry mass	$6.58 \pm 1.21 \times 10^{-10}$	mg $cell^{-1}$	This study
μ (75 °C)	Water dynamic viscosity	3.69×10^{-4}	kg m^{-1} s^{-1}	(CRC, 2003)
μ (30 °C)		7.77×10^{-4}	kg m^{-1} s^{-1}	
L_b	Boundary layer thickness	10	μm	This study
S_s	Supernatant substrate concentration	0	g L^{-3}	This study
X_p	Planktonic cell concentration	1.10×10^7	cells ml^{-1}	This study
X_b	Boundary layer cell concentration		cells ml^{-1}	This study
η	Effectiveness factor			(Grady et al., 1999)
η^*	Modified effectiveness factor			This study

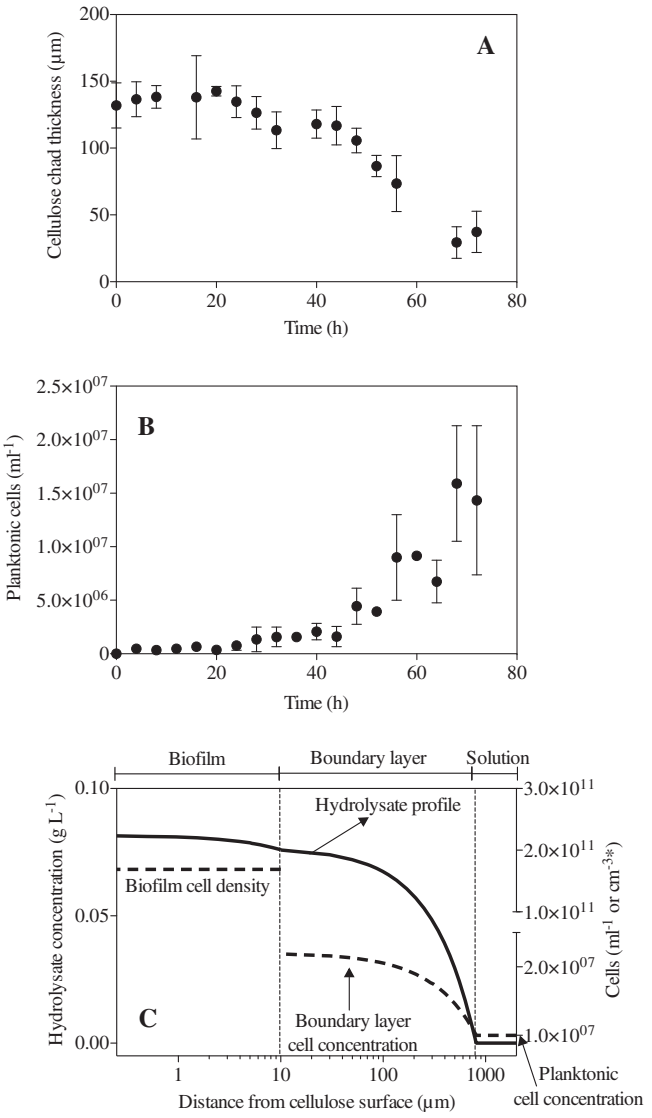

Fig. 2. Fermentation of cellulose chads by *C. obsidiansis* in serum bottles, (A) The reduction of cellulose chad thickness over time and (B) the increase in planktonic cells over time; (C) Hydrolysate concentration and cell number in the biofilm and boundary layer as simulated by the hydrolysate diffusion and utilization model, * unit for biofilm cell density, the *X*-axis is plotted in log-scale.

$$(J_{in} - J_{b-out})Y_{obs} = \rho_x L_f \mu_f \quad (15)$$

3.3. Hydrolysate flux

The results of the hydrolysate diffusion and utilization simulations over of the range of boundary layer thicknesses (L_b) show a positive relationship between L_b and μ_f, such that a thicker boundary layer helps the biofilm retain more hydrolysate in terms of $(J_{in} - J_{f\text{-}out})/J_{in}$ in the course of diffusion, and thus gives rise to a faster μ_f (Table 2). This positive relationship differs from models based on biofilm growth on a soluble substrate in which L_b plays a negative role and must be attenuated with intensive shear force (Grady et al., 1999). The role of the boundary layer in retaining hydrolysate within the biofilm may account for the differing impacts of L_b on cellulolytic biofilms versus biofilms grown on soluble substrates (Fig. 1). Experimental data indicating that the cellulolytic biofilm reaches and maintains a constant thickness (around 10 μm) suggests a mass balance has been reached between the rate of cell growth and detachment (data not shown). Based on these data, the specific growth rate of the biofilm can be inferred from its specific detachment rate determined experimentally as $\mu_f = 0.13\ h^{-1}$ according to Eq. (16),

$$\mu_f = \frac{R_{det} V}{\rho_x L_f A} \quad (16)$$

Comparing this calculated μ_f value derived from experimental data to the L_b-dependent simulated μ_f values reported in Table 2, a boundary layer value of 800 μm appears to be an appropriate thickness for the *C. obsidiansis* biofilm growing on a cellulose chad. This value is consistent with typical L_b values reported in bioreactors ranging from 100 to 1200 μm (Bishop et al., 1997). Although the estimated boundary layer thickness is within this range, it may be larger than expected in this study for the following reasons. First, in this experimental design, the cell culture was grown with moderate shaking (100 rpm) compared to the more vigorous mixing conditions in a mechanically mixed bioreactor. Second, the boundary layer is predicted to increase with the suspended particle size, so the size of the cellulose chad (7.37 ± 0.03 μm in diameter) may artificially result in an larger L_b. Third, according to the Stokes–Einstein equation, the mass diffusion coefficient is doubled and the water viscosity is halved at 75 °C (Table 1), which allows for greater diffusion distance in the boundary layer. Lastly, cellobiose, the substrate used in this study, gives the greatest mass diffusion coefficient among all cellodextrins due to its small molecular size, which may also lead to an overestimation of the boundary layer thickness (Kurath and Swanson, 1961).

The simulations based on this experimental design (Table 2) predict that only 11% of the hydrolysate will be utilized by a cellulolytic biofilm grown to a thickness of 10 μm despite the high cell density. A small fraction of the hydrolysate would be consumed in the boundary layer and the remaining sugars (88%) would diffuse through the biofilm into the bulk solution (Table 2). The phenomenon of hydrolysate efflux through the biofilm indicated by an increased concentration of sugar in the bulk liquid has been observed in many other cellulose fermentations (Lo et al., 2009; Lu et al., 2006). This hydrolysate efflux suggests that the rate of substrate utilization by the surface adhered cells is slower than the rate of diffusion of soluble sugars out of the biofilm.

3.4. Hydrolysate concentration

A simulation of the hydrolysate profile across the biofilm and boundary layer is presented in Fig. 2C. This simulation shows a diffusion profile with the maximum hydrolysate concentration at the cellulose surface and the minimum concentration in bulk solution. The motive force maintaining this gradient is microbial cellulose degradation at the cellulose surface which produces hydrolysate

Table 2
Prediction of hydrolysate flux and utilization in cellulolytic biofilm formed on cellulose chad at various L_b.

L_b (μm)	J_{in} (g cm^{-2} h^{-1})	$J_{f\text{-}out}$ (g cm^{-2} h^{-1})	$J_{b\text{-}out}$ (g cm^{-2} h^{-1})	$(J_{in} - J_{f\text{-}out})/J_{in}$ (%)	$(J_{f\text{-}out} - J_{b\text{-}out})/J_{in}$ (%)	$J_{b\text{-}out}/J_{in}$ (%)	μ_f (h^{-1})
8	5.33×10^{-5}	5.29×10^{-5}	5.29×10^{-5}	0.75	0.00	99.25	0.01
80	5.33×10^{-5}	5.23×10^{-5}	5.23×10^{-5}	1.88	0.00	98.12	0.02
800	5.33×10^{-5}	4.72×10^{-5}	4.71×10^{-5}	11.44	0.19	88.37	0.13

at a rate of $J_{in} = 5.33 \times 10^{-5}$ g cm^{-2} h^{-1} that diffuses into the biofilm (Table 2). The extensive efflux ($J_{b\text{-}out}$ in Table 2) indicates that the thin cellulolytic biofilm is incapable of consuming all of the hydrolysate influx. As a consequence, the hydrolysate diffuses through the biofilm and gives rise to an efflux of $J_{f\text{-}out}$ into the boundary layer. Although up to 2×10^7 *C. obsidiansis* cells ml^{-1} are distributed in the boundary layer, the amount of substrate utilized by growing cells in the boundary layer is minimal compared to the total influx. For this reason, 88% of the hydrolysate escapes into the bulk solution (Table 2). The hydrolysate concentration profile is quite uniform across the biofilm (Fig. 2C) implying a uniform growth rate would result with respect to film thickness. Moreover, this uniform hydrolysate profile suggests that the hydrolysate influx exceeds the hydrolysate utilization capacity of the biofilm despite its high cell density, i.e., the rate-limiting step for cellulolytic biofilm growth lies in its substrate utilization rather than hydrolysis (Fig. 2C). Consistent with previous reports (van Loosdrecht et al., 2002), the rate-limitation in substrate utilization may explain the homogeneous thin biofilm morphology observed microscopically (data not shown).

3.5. Verification of the hydrolysate efflux from the cellulolytic biofilm

Due to the minimal initial substrate concentrations in the cellulose chad experiment, no measurable sugar concentration could be detected in the supernatant, even though it is predicted in the model simulation (data not shown). In order to test whether hydrolysate efflux was occurring during biofilm growth, *C. obsidiansis* was grown in the presence of a larger amount of initial feedstock (30 g L^{-1} Avicel) and the fermentation was followed for 120 h (Fig. 3). Like previous experiments, a constant Avicel hydrolysis rate was observed, which was independent of the planktonic cell concentration which increased from 10^7 to 10^9 cell ml^{-1} over the course of the experiment (Fig. 3A). Because planktonic cells quickly consume any hydrolysate that diffuses through the biofilm into the bulk liquid, it is hypothesized that the presence of leaked hydrolysate in the bulk liquid may be detectable only in the early stages of batch fermentation when the planktonic cell concentration is low. To test this, the reducing sugar and planktonic cell concentrations were measured during early and mid-log-phase growth. As predicted, an accumulation of reducing sugar in the bulk liquid was observed during the first 5 h of the fermentation when the planktonic cell concentration was below 5×10^7 cells ml^{-1} (Fig. 3B). As the planktonic cell concentration increased, reducing sugars in the bulk liquid were no longer detected during the log phase, suggesting that the soluble substrate was consumed by planktonic cells (Fig. 3B). Similar soluble carbohydrate profiles have been reported during Avicel fermentation by other cellulolytic microorganisms (Lu et al., 2006). It is important to note that at later stages of the fermentation process, substrate hydrolysis by the biofilm becomes the overall rate-limiting step when considering the biofilm and planktonic cells as a whole system, which is consistent with published reports (Lynd et al., 2002).

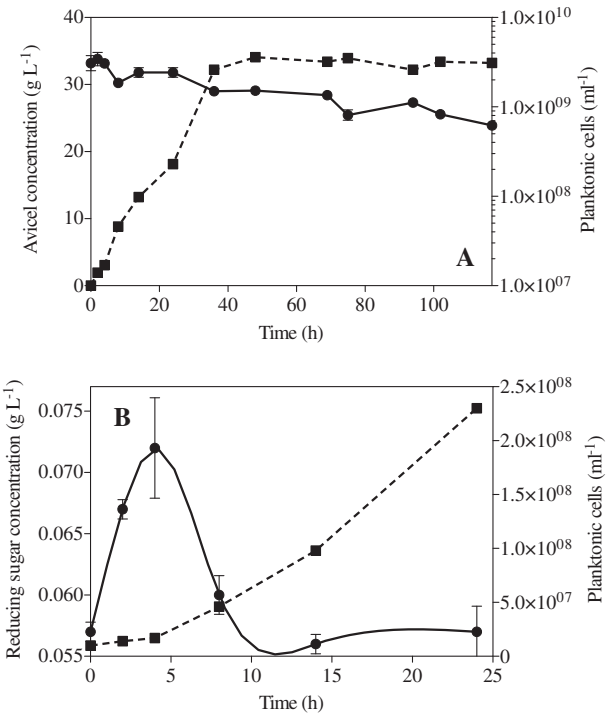

Fig. 3. Fermentation of Avicel by *C. obsidiansis* in a bioreactor, (A) Concentration profiles of Avicel (●) and planktonic cells (■); (B) Concentration profiles of reducing sugar (●) and planktonic cells (■) during early and mid-log-phase growth.

3.6. Why does a hydrolysate efflux occur in a cellulolytic biofilm?

Both model analysis and experimental results indicate that the cellulolytic biofilm consumes only a fraction of the hydrolysate generated by microbial hydrolysis and the rest of the hydrolysate diffuses into the bulk liquid. The hydrolysate "leakage" is often observed in cellulose fermentation (Lo et al., 2009; Lu et al., 2006) and was originally inferred from the cross-feeding phenomenon. As early as the 1950s, it was recognized that starch-digesting ruminal bacteria outnumbered cellulolytic bacteria in cattle rumen despite the fact that the cattle's diet was primarily cellulose (Bryant and Burkey, 1953). Later, Scheifinger and Wolin (1973) demonstrated successful co-cultivation of a cellulolytic and a non-cellulolytic bacterial species with cellulose as the sole carbon source, and the two microbes were found at roughly equal numbers. Russell (1985) subsequently showed that cellodextrins generated by cellulolytic bacteria were consumed by the non-cellulolytic microbial species. Interestingly, cross-feeding between pure cultures of attached and non-attached cells similar to the finding in this study was also observed previously (Wells et al., 1995). Results from this study indicate that a hydrolysate concentration gradient must exist between the cellulolytic biofilm and the bulk solution to ensure a high enough intra-biofilm hydrolysate concentration for biofilm growth (Fig. 2C). This gradient is maintained by the continuous hydrolysate efflux from the biofilm and is particularly important when the carbohydrate concentration in the bulk solution is low (Fig. 2C). In a natural system, one would expect the hydrolysate concentration in the bulk solution to be low as non-cellulolytic microbes consume soluble compounds (Johnson et al., 1985). As a consequence, the main mechanism to produce a hydrolysate concentration gradient compatible with cellulolytic biofilm growth is to allow hydrolysate diffusion out of the biofilm into the bulk liquid.

One question that still remains is whether conditions exist in which hydrolysate efflux does not occur, i.e., hydrolysate diffusion but not utilization becomes the rate-limiting step for cellulolytic biofilm growth. The model system developed in this study may provide some insight into this question. Effectiveness factor (η) is a routine indicator used to evaluate whether a biofilm is subjected to substrate utilization or diffusion limitation (Grady et al., 1999). It is defined as the ratio of the bioreaction rate under diffusion limiting and non-limiting conditions. η gives a value of approximately 1 when substrate utilization is the rate limiting determinant and a value less than 1 when diffusion is the limiting factor. However, this indicator does not apply to cellulolytic biofilms in which the mass diffusion limitation starts to play a significant role as mentioned above, i.e., diffusion resistance helps hold more hydrolysate

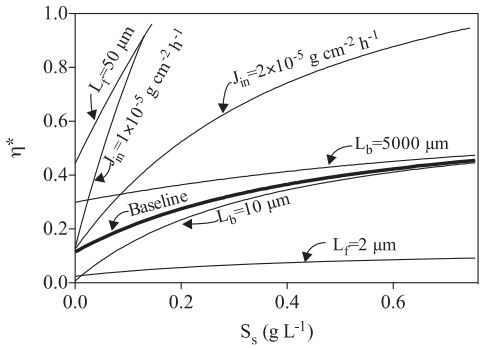

Fig. 4. Effects of J_{in}, S_s, L_f and L_b on η^*, baseline is simulated with major parameters adapted from Fig. 2C, i.e., $J_{in} = 5.33 \times 10^{-5}$ g cm^{-2} h^{-1}, $L_f = 10$ μm, $L_b = 800$ μm. The other profiles were simulated with one parameter change at a time to see the parameter's effect.

within the biofilm for higher substrate utilization rate. This positive effect of diffusion limitation in a cellulolytic biofilm will lead to $\eta > 1$, implying η has lost its original physical meaning defined for a biofilm grown on a soluble substrate diffused from bulk solution. For this reason, a modified effectiveness factor (η^*) is defined to evaluate the relative contributions of substrate utilization and diffusion rates in a cellulolytic biofilm,

$$\eta^* = \frac{\text{Hydrolysate utilization rate per surface area}}{\text{Hydrolysate influx rate per surface area}} = \frac{\int_0^{L_f} \frac{\mu_{max} S}{K_s + S} \frac{\rho_x}{Y_{obs}} dL}{J_{in}} \quad (17)$$

In this equation, η^* is a dimensionless parameter. When $\eta^* < 1$, substrate utilization is the rate-limiting step for biofilm growth. When cellulose is the sole carbon source, J_{in} should be the upper-limit of the hydrolysate utilization rate in the biofilm, and thus only $\eta^* \leqslant 1$ is possible. This means that a cellulolytic biofilm cannot have a theoretical substrate utilization rate that exceeds the substrate diffusion rate. However, conditions may exist in which η^* approaches 1 when the process is close to the diffusion limitation. To determine which parameters impact the value of η^* most significantly, the effects of J_{in}, S_s, L_f and L_b on the value of η^* were simulated with reference to a baseline established with parameters adapted from Fig. 2C. Each profile is simulated with a single parameter varied at a time so that the effect of each parameter can be compared. These simulations indicate that all parameters except J_{in} play a positive role on η^*, although with different sensitivities (Fig. 4). η^* appears to be more sensitive to changes in L_f and J_{in} but less to L_b as S_s increases. For example, η^* quickly approaches a value of 1 when L_f increases 5-fold or J_{in} decreases 5-fold with respect to the baseline. In contrast, a 500-fold change in L_b does not significantly impact the value of η^* (Fig. 4). Although S_s is simulated with a range of K_s values in Fig. 4, only supernatant carbohydrate concentrations lower than 0.2 g L^{-1} are typical in cellulose fermentors, probably owing to the quick consumption by planktonic cells. The results from these simulations indicate that the only possibility for η^* to approach 1 within the typical S_s range is by a reduction in J_{in} or with a thicker biofilm (L_f). A reduced rate of cellulose hydrolysis ($J_{in} < 10^{-5}$) is typically associated with less-biodegradable substrates, such as crystalline cellulose (Fig. 4). Under these conditions, the rate of substrate utilization may be constrained by the rate of substrate diffusion (Fig. 4).

4. Conclusions

The hydrolysate flux and utilization in a cellulolytic biofilm formed on a cellulose surface was evaluated with the model system developed in this study. The data indicate that a thin cellulolytic biofilm apparently must generate more hydrolysate than consumed. This is necessary to establish a soluble substrate concentration that is higher than that of the bulk solution, which therefore supports biofilm growth. This concentration gradient is maintained by a cellulose hydrolysis rate that is greater than the utilization rate. In this sense, there exists a hydrolysate surplus and thus, the hydrolysate utilization rate in a cellulolytic biofilm becomes its major growth-limiting factor. These results may also apply to other microbes that form thin biofilms on insoluble substrates, although this remains to be tested.

Acknowledgements

This work was supported by the BioEnergy Science Center (BESC), which is a US Department of Energy Bioenergy Research Center supported by the Office of Biological and Environmental Research in the DOE Office of Science. Oak Ridge National Laboratory is managed by UT-Battelle, LLC, for the US Department of Energy under contract DE-AC05-00OR22725.

References

APHA, 1998. Standard Methods for the Examination of Water and Wastewater, 20th ed. American Public Health Association, Washington DC, USA.
Bayer, E., Shoham, Y., Lamed, R., 2006. Cellulose-decomposing bacteria and their enzyme systems. Prokaryotes 2, 578–617.
Bishop, P.L., Gibbs, J.T., Cunningham, B.E., 1997. Relationship between concentration and hydrodynamic boundary layers over biofilms. Environ. Technol. 18, 375–385.
Bryant, M.P., Burkey, L.A., 1953. Numbers and some predominant groups of bacteria in the rumen of cows fed different rations. J. Dairy Sci. 36, 218–224.
CRC, 2003. Handbook of Chemistry and Physics, 84th ed. Chemical Rubber Company, Cleveland, Ohio.
Fan, L.S., Leyva-Ramos, R., Wisecarver, K.D., Zehner, B.J., 1990. Diffusion of phenol through a biofilm grown on activated carbon particles in a draft-tube three-phase fluidized-bed bioreactor. Biotechnol. Bioeng. 35, 279–286.
Grady, C.P.L., Daigger, G.T., Lim, H.C., NetLibrary Inc., 1999. Biological Wastewater Treatment, 2nd ed. Marcel Dekker, New York.
Hamilton-Brehm, S.D., Mosher, J.J., Vishnivetskaya, T., Podar, M., Carroll, S., Allman, S., Phelps, T.J., Keller, M., Elkins, J.G., 2010. *Caldicellulosiruptor obsidiansis sp. Nov.*, an anaerobic, extremely thermophilic, cellulolytic bacterium isolated from Obsidian Pool, Yellowstone National Park. Appl. Environ. Microb. 76, 1014–1020.
Himmel, M.E., Xu, Q., Luo, Y.H., Ding, S.Y., Lamed, R., Bayer, E.A., 2010. Microbial enzyme systems for biomass conversion: emerging paradigms. Biofuels 1, 323–341.
Jensen, P.D., Hardin, M.T., Clarke, W.P., 2009. Effect of biomass concentration and inoculum source on the rate of anaerobic cellulose solubilization. Bioresour. Technol. 100, 5219–5225.
Johnson, E.A., Bouchot, F., Demain, A.L., 1985. Regulation of cellulase formation in *Clostridium thermocellum*. J. Gen. Microbiol. 131, 2303–2308.
Kim, Y.C., 1996. Diffusivity of bacteria. Korean J. Chem. Eng. 13, 282–287.
Kurath, S.F., Swanson, J.W., 1961. The Molecular Properties of Naturally Occurring Polysaccharides. The Effect of Ion Binding on the Molecular Properties of Low Molecular Weight Polysaccharides. Project 2236, Report Four to the Pioneering Research Committee, Pioneering Research Program. The institute of paper chemistry, Appleton, Wisconsin.
Lo, Y.C., Su, Y.C., Chen, C.Y., Chen, W.M., Lee, K.S., Chang, J.S., 2009. Biohydrogen production from cellulosic hydrolysate produced via temperature-shift-enhanced bacterial cellulose hydrolysis. Bioresour. Technol. 100, 5802–5807.
Lu, Y.P., Zhang, Y.H.P., Lynd, L.R., 2006. Enzyme-microbe synergy during cellulose hydrolysis by *Clostridium thermocellum*. Proc. Natl. Acad. Sci. USA 103, 19605.
Lynd, L.R., Laser, M.S., Brandsby, D., Dale, B.E., Davison, B., Hamilton, R., Himmel, M., Keller, M., McMillan, J.D., Sheehan, J., Wyman, C.E., 2008. How biotech can transform biofuels. Nat. Biotechnol. 26, 169–172.
Lynd, L.R., Weimer, P.J., van Zyl, W.H., Pretorius, I.S., 2002. Microbial cellulose utilization: fundamentals and biotechnology. Microbiol. Mol. Biol. Rev. 66, 506–577.
Miller, G.L., 1959. Use of dinitrosalicylic acid reagent for determination of reducing sugar. Anal. Chem. 31, 426–428.
Miron, J., Ben-Ghedalla, D., Morrison, M., 2001. Invited review: adhesion mechanisms of rumen cellulolytic bacteria. J. Dairy Sci. 84, 1294–1309.
O'Sullivan, C., Burrell, P.C., Pasmore, M., Clarke, W.P., Blackall, L.L., 2009. Application of flow cell technology for monitoring biofilm development and cellulose degradation in leachate and rumen systems. Bioresour. Technol. 100, 492–496.
Park, Y.S., Yun, J.W., Song, S.K., 1998. Biofilm properties under different substrate loading rates in a rotating biological contactor. Biotechnol. Tech. 12, 587–590.

Rittmann, B.E., McCarty, P.L., 2001. Environmental Biotechnology: Principles and Applications. McGraw-Hill, Boston.
Russell, J.B., 1985. Fermentation of cellodextrins by cellulolytic and noncellulolytic rumen bacteria. Appl. Environ. Microb. 49, 572–576.
Scheifinger, C.C., Wolin, M.J., 1973. Propionate formation from cellulose and soluble sugars by combined cultures of *Bacteroides succinogenes* and *Selenomonas ruminantium*. Appl. Microbiol. 26, 789–795.
Stewart, P.S., 1998. A review of experimental measurements of effective diffusive permeabilities and effective diffusion coefficients in biofilms. Biotechnol. Bioeng. 59, 261–272.
Trulear, M.G., Characklis, W.G., 1982. Dynamics of biofilm processes. J. Water Pollut. Control Fed. 54, 1288–1301.
van Loosdrecht, M.C.M., Heijnen, J.J., Eberl, H., Kreft, J., Picioreanu, C., 2002. Mathematical modelling of biofilm structures. Antonie van Leeuwenhoek 81, 245–256.
Wang, Z.W., Chen, S.L., 2009. Potential of biofilm-based biofuel production. Appl. Microbiol. Biotechnol. 83, 1–18.
Weimer, P.J., Hatfield, R.D., Buxton, D.R., 1993. Inhibition of ruminal cellulose fermentation by extracts of the perennial legume cicer milkvetch (*Astragalus cicer*). Appl. Environ. Microbiol. 59, 405–409.
Wells, J.E., Russell, J.B., Shi, Y., Weimer, P.J., 1995. Cellodextrin efflux by the cellulolytic ruminal bacterium *Fibrobacter succinogenes* and its potential role in the growth of nonadherent bacteria. Appl. Environ. Microb. 61, 1757–1762.